

## Co-Re-based alloys a new class of material for gas turbine applications at very high temperatures

D. Mukherji<sup>\*1</sup>, J. Rösler<sup>1</sup>, J. Wehrs<sup>1</sup>, H. Eckerlebe<sup>2</sup> and R. Gilles<sup>3</sup>

<sup>1</sup>*TU Braunschweig, Institut für Werkstoffe, Braunschweig, Germany*

<sup>2</sup>*Helmholtz-Zentrum Geesthacht, Geesthacht, Germany*

<sup>3</sup>*TU München, Forschungs Neutronenquelle Heinz Maier-Leibnitz (FRM II), Garching, Germany*

*(Received April 18, 2012, Revised July 24, 2012, Accepted August 14, 2012)*

**Abstract.** Co-Re alloy development is prompted by the search for new materials for future gas turbines which can be used at temperatures considerably higher than the present day single crystal Ni-based superalloys. The Co-Re based alloys are designed to have very high melting range. Although Co-alloys are used in gas turbine applications today, the Co-Re system was never exploited for structural applications and basic knowledge on the system is lacking. The alloy development strategy therefore is based on studying alloying additions on simple model alloy compositions of ternary and quaternary base. Various strengthening possibilities have been explored and precipitation hardening through fine dispersion of MC type carbides was found to be a promising route. In the early stages of the development we are mainly dealing with polycrystalline alloys and therefore the grain boundary embrittlement needed to be addressed and boron addition was considered for improving the ductility. In this paper recent results on the effect of boron on the strength and ductility and the stability of the fine structure of the strengthening TaC precipitates are presented. In the beginning the alloy development strategy is briefly discussed.

**Keywords:** Co-base alloy; rhenium; boron; small-angle X-ray scattering; diffraction

---

### 1. Introduction

Materials are used in modern gas turbines in the most stringent conditions of temperature and loading and Ni-based alloys are the dominant material class in this application. Ever since the introduction of the first  $\gamma/\gamma'$  based Ni-alloy just after the Second World War, there is a remarkable development in this class of alloys which has come to be known as the superalloys. In the same period there was also a tremendous increase in the gas temperature inside the turbines and it is envisaged that future turbines will operate at even higher temperatures. Fig. 1 presents the evolution in the temperature capability of the superalloys (measured by 1000 h creep life under the stress of 137 MPa) and aircraft gas turbines (measured in terms of the Take-off turbine entry temperature TET) over the last 60 to 70 years. These are typical data from specific alloys and specific aeroengines but they quite well represent the trends in the development. The information is collected from various sources to plot Fig. 1 (e.g. Perepezko 2009, Reed 2006). Ni-superalloys went through considerable evolution from wrought to conventionally cast to directional solidification to

---

\*Corresponding author, Ph. D., E-mail: [d.mukherji@tu-bs.de](mailto:d.mukherji@tu-bs.de)

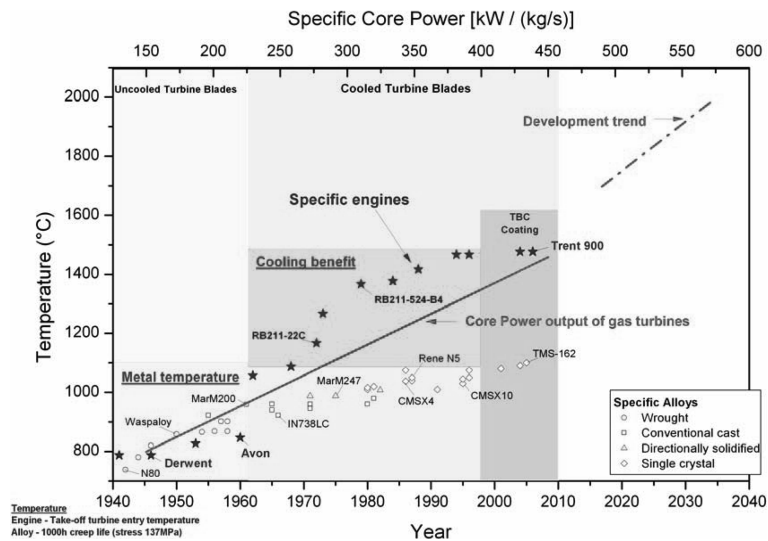


Fig. 1 Evolution of the high temperature capability of the Ni-based superalloys in the last 70 years. The figure also includes the evolution of the turbine entry temperatures at take-off for specific civil aeroengines

single crystal turbine blades which yielded a 250°C increase in allowable metal temperature (Miller 1996). Further, blade cooling and the use of thermal barrier coatings (TBC) have also added tremendously (several hundred °C), allowing turbine gas entry temperature to reach nearly 1500°C today (Fig. 1, e.g. 1480°C in the Trent 900 engines introduced in 2006 by Rolls Royce) (Reed 2006). It is estimated that over the next twenty years a further 200°C increase in turbine entry gas temperature will be required for improved performance (Miller 1996).

Since the Ni-superalloys are already used very close to their melting point ( $> 0.8 T_M$ ) it is not envisaged that they can meet this future demand of gas turbines although material development will continue to push the maximum service temperature of Ni-superalloys upwards. Therefore, the development of new material is essential in order to find a solution beyond the Ni-based superalloys. We view that a key criterion for any future high temperature material is to have a very high melting temperature and high temperature stability. With this in mind we introduced the Co-Re based alloys in 2007 (Rösler *et al.* 2007). The addition of the refractory metal Rhenium can increase the melting temperature of Co-alloys significantly. The aim is to develop high temperature alloys for applications at bare metal temperature of 1200°C.

In this paper we first briefly present our alloy development strategy and then some selected results from different microstructural and crystallographic characterization.

## 2. Alloy development strategy

Co-based alloys are not new and are presently used in gas turbines for static parts up to 1000°C. There is even a new development trend in Co-Al-W alloys (Sato *et al.* 2006) to produce a  $\gamma/\gamma'$  structure (fcc /  $L1_2$ ) similar to that in Ni-superalloys to improve strength. However, this development

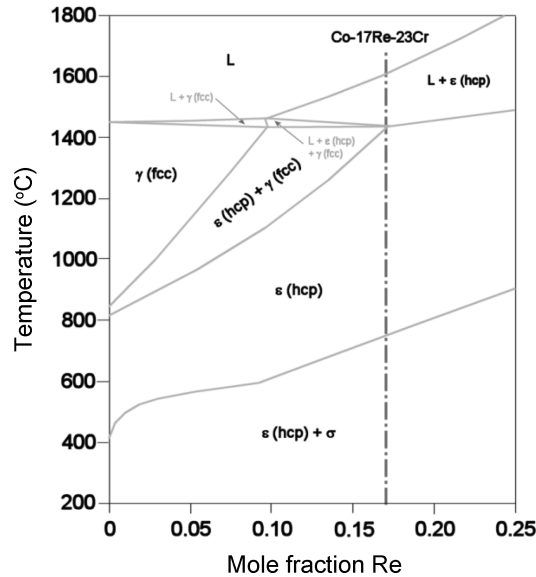


Fig. 2 Thermodynamically calculated isoplethal section of the Co-23Cr + Re (0-25 at.%). The dotted vertical line marks the Co-17Re-23Cr alloy position in this diagram

does not promise higher application temperatures than Ni-superalloys. Whereas, in the Co-Re system it is possible to suitably adjust the melting range by the amount of *Re* addition. The refractory metal *Re* has the third highest melting point (3182°C; only carbon and tungsten have higher melting points) amongst all elements, which is more than double the melting points of *Co* (1495°C) and *Ni* (1453°C). Moreover, *Re* dissolves readily in *Co* and a complete miscibility exists in the Co-Re binary system. It is therefore, possible to continuously increase the melting temperature of *Co* alloys with the addition of *Re*. The Co-17Re-23Cr alloy<sup>1</sup> is the reference system in our alloy development. *Cr* addition in the range of 23 at.% does not significantly affect the *Co* melting temperature and there is only a marginal decrease as can be seen in Co-Cr binary phase diagram (Okamoto 2003) but about 17 at.% *Re* addition in *Co* can raise the liquidus temperature significantly, from 1495°C in pure *Co* to ~1700°C in Co-17Re as can be seen from the Co-Re binary phase diagram (Massalski 1986). In the experimental Co-Re alloys both *Cr* and *Re* addition stabilizes the hexagonal close packed (hcp)  $\epsilon$  *Co* phase as the matrix, which is also the thermodynamically stable low temperature allotromorph of *Co*. However, in pure *Co* and in conventional Co-alloys, the high temperature face centred cubic (fcc)  $\gamma$  *Co* phase is retained at room temperature (RT) either as a metastable phase or through alloying addition (e.g. *Ni*). This distinguishes Co-Re base alloys from the conventional *Co* alloys and it required a new approach in the Co-Re alloy development.

Numerical modelling of phase equilibria in ternary and multi-component Co-Re systems was extensively used in our study. The software package ThermoCalc using the TTNi7 database established by Thermotech Ltd. (Lukas *et al.* 2007) was the main tool for these calculations. The thermodynamically calculated isoplethal section of Co-23Cr with varying *Re* content (0 to 25 at.%) is presented in Fig. 2.

<sup>1</sup>All compositions in this paper are given in atomic percent (at. %) except for *B* content which is expressed in parts per million by weight (*wt. ppm*).

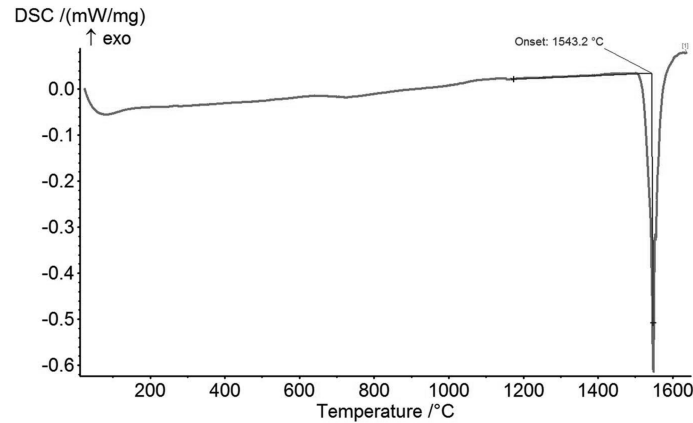


Fig. 3 DSC measurement showing melting peak in Co-17Re-23Cr alloy during heating. Heating rate was 10 K/min

The plot of the vertical section include the composition of the Co-17Re-23Cr alloy and shows that for this alloy the liquidus temperature is at  $\sim 1600^{\circ}\text{C}$ . It was discussed in an earlier publication that due to the use of TTNI7 database (which is essentially a Ni-alloy database validated for *Re* content up to only 7%) in our thermodynamic calculations the high temperature phase boundaries may not have been accurately determined (Mukherji *et al.* 2012a). Therefore the melting ranges in Co-Re alloys were actually verified experimentally through differential scanning calorimetry (DSC) and differential thermal analysis (DTA) measurements and the DSC result for Co-17Re-23Cr alloy is shown in Fig. 3. The onset of melting during heating (@ 10 K/min) in Co-17Re-23Cr alloy lies at  $1543^{\circ}\text{C}$  in this measurement, which is an indicator of the solidus temperature. Clearly, the Co-Re alloys have much higher melting points than Ni-superalloys.

The Co-Re system has not been studied widely in the past, particularly mechanical property and oxidation data are scanty. Few literature reports that exist mainly relate to crystallographic investigations and phase diagrams (e.g. Sokolovskaya 1986). Exploiting Co-Re alloys for structural application, therefore, needed a more fundamental approach. In order to gain basic understanding of the Co-Re system we first studied the effect of different alloying elements on strength and oxidation using model alloy compositions of ternary or quaternary systems. Alloys were designed to study strengthening mechanisms (Mukherji *et al.* 2010a, Heilmaier 2009, Mukherji and Rösler 2010b, Mukherji *et al.* 2010c) like precipitation hardening by carbides ( $\text{M}_{23}\text{C}_6$  and MC types), solid-solution hardening by large atoms (e.g. Re) or composite strengthening with second phase ( $\sigma$  phase) on the one side and oxide formation and oxidation behaviour (Klauke *et al.* 2009, Gorr *et al.* 2009) on the other side. Moreover, preliminary investigation on cast polycrystalline Co-Re alloys showed that grain boundary embrittlement is a critical issue and it limits both the strength and the ductility of the alloys at room and high temperatures. Addition of *B* in small amounts (50 to 1000 ppm by weight) to Co-Re alloys produced dramatic improvement in properties (Mukherji *et al.* 2012b).

*Cr* which promotes the formation of a protective  $\text{Cr}_2\text{O}_3$  oxide layer in conventional iron, nickel and cobalt alloys was however, not that effective in Co-Re alloys and only in conjunction with *Si* provided good oxidation resistance to  $1100^{\circ}\text{C}$  (Gorr *et al.* 2009). For further improvement in oxidation behaviour needed at higher temperatures, addition of *Al* is being considered.

Table 1 Comparison of mechanical properties of polycrystalline Co-17Re-23Cr + 200B alloy with single crystal Ni-base superalloy CMSX4 at RT

Alloy	Density ( $\rho$ ) g / cc	UTS ( $\sigma$ ) MPa	Specific strength ( $\sigma / \rho$ )	Ductility ( $\epsilon$ ) %
Co-17Re-23Cr + 500B	11.5	1276	110.9	20.3
CMSX4	8.7	894	102.7	22

### 3. Effect of boron on strength and ductility

The reference ternary alloy Co-17Re-23Cr is an experimental alloy of the Co-Re system where Cr is primarily added to improve the oxidation behaviour of the alloy. However, addition of > 20% Cr to Co-Re alloys can stabilize a significant amount of the topologically closed packed (tcp)  $\sigma$  phase. The  $\text{Cr}_2\text{Re}_3$  type  $\sigma$  phase (sp. gp. no. 136) has a very high strength (hardness of above 1200 HV10), but it is also a very brittle phase. The Co-17Re-23Cr alloy has good strength, but its ductility in polycrystalline state is extremely poor. Investigation has confirmed that the  $\sigma$  phase present in large sizes ( $> 5 \mu\text{m}$ ) as in ST<sup>2</sup> heat treated Co-17Re-23Cr alloy may develop cracks within them when the alloy is deformed, but this is not the cause for the brittleness of the alloy as failure occurs at grain boundaries with a brittle inter-granular fracture (Mukherji *et al.* 2012b). Further, when the  $\sigma$  phase morphology is refined (e.g. in Co-17Re-23Cr-15Ni alloy through Ni addition and suitable heat treatment) to a fine dispersion (size of about 100 nm) this phase is no more brittle (Mukherji *et al.* 2010d). It was also shown that B addition has a pronounced beneficial effect on the mechanical properties of the polycrystalline Co-17Re-23Cr alloy at all temperatures (Mukherji *et al.* 2012b). Only a small amount of B, as low as 500 wt. ppm, drastically improves both the strength and ductility such that the polycrystalline alloy Co-17Re-23Cr+500B at RT has a specific strength comparable to the single crystal Ni-superalloy CMSX 4, despite its much higher density. A comparison of strength ( $\sigma$ ), density ( $\rho$ ) and specific strength ( $\sigma / \rho$ ) of the Co-17Re-23Cr+500B and CMSX4 alloys is shown in Table 1.

The strength of the Co-17Re-23Cr alloy is dependent on the boron amount and the hardness plot in Fig. 4 shows that the strength peaks at B content around 200 ppm (see plot HV10). The HV10 hardness numbers are obtained using a 10 kg load and the indentation is large enough to cover several grains and cross grain boundaries (Fig. 5a). To check the strength of the matrix a lower loads of 1 kg and 300 g were used to measure hardness within the grains. The results are also plotted as HV1 and HV0.3 values in Fig. 4 which shows less or no dependence on the boron content of the alloy. The scatter in HV1 values are high and this is because the indentation some time includes hard  $\sigma$  particles which are present within the grains (Fig. 5b). However, lowering the load to 300 g makes it possible to measure the hardness of the Co-matrix alone and in Fig. 4 it can be seen that the linear fit to the HV0.3 data is horizontal. Fig. 5c shows a typical hardness indentation with 300 g load. Positions of these low load indentations (HV0.3) were carefully chosen such that they do not cross grain boundaries, nor they touch any  $\sigma$  phase particle. So essentially, the HV0.3 values are typical hardness of the Co-solid solution matrix. The slip lines associated with the indentation (Fig. 5c) shows that the matrix is quite ductile. It is apparent that the Co-matrix strength is independent of the B content in the alloy. The results suggest that boron segregates to the grain boundaries. In

<sup>2</sup>ST (solution treatment) in Co-17Re-23Cr alloy = 1350°C / 5 h + 1400°C / 5 h + 1450°C / 5 h in vacuum and fast cool in high pressure argon.

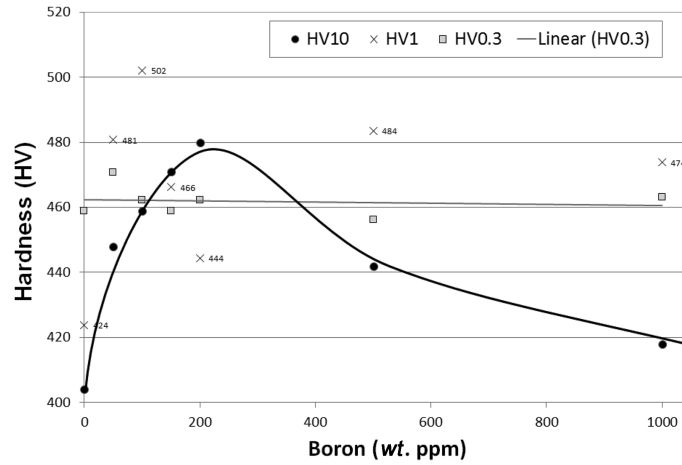


Fig. 4 Hardness values measured with different loads on Co-17Re-23Cr alloy with varying boron content after the ST heat treatment. Trend lines are plotted for the HV10 and HV0.3 data points. The crosses (x) mark the random scatter in the HV1 data points where the hardness values are also shown

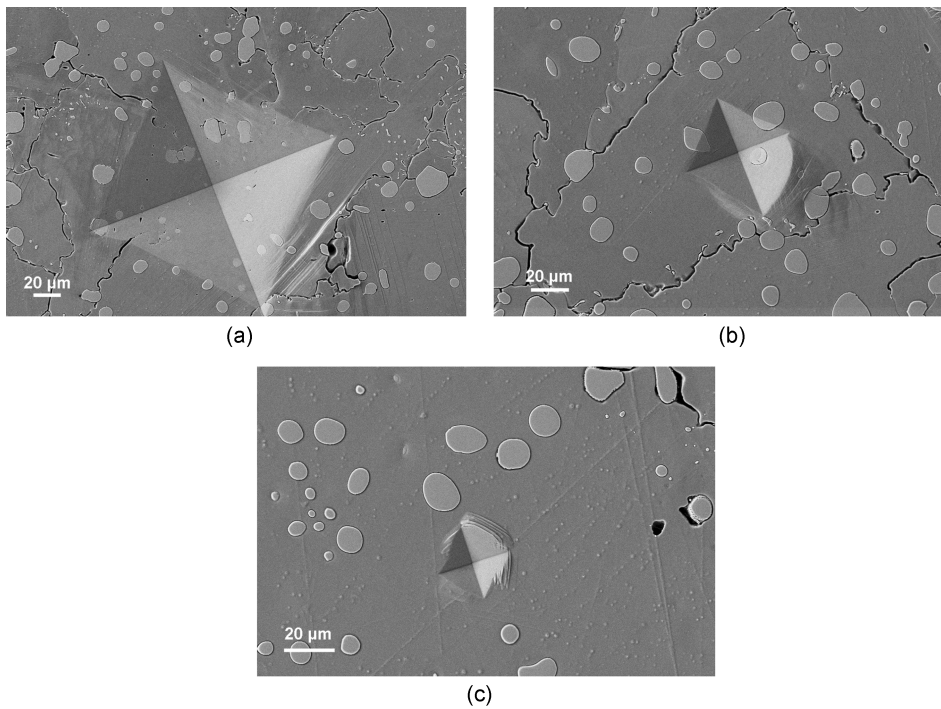


Fig. 5 Typical SEM images of the hardness indentation marks on Co-17Re-23Cr alloy with or without boron using different loads: (a) 10 Kg, (b) 1 Kg and (c) 300 g

fact it has been seen that Boron addition stabilizes  $\text{Cr}_2\text{B}$ -type Cr-Re boride phase which decorates the grain boundaries (Böhlitz *et al.* 2012). The amount of boride increases with the  $B$  content in the alloy (Mukherji *et al.* 2012b, Mukherji *et al.* 2010d).

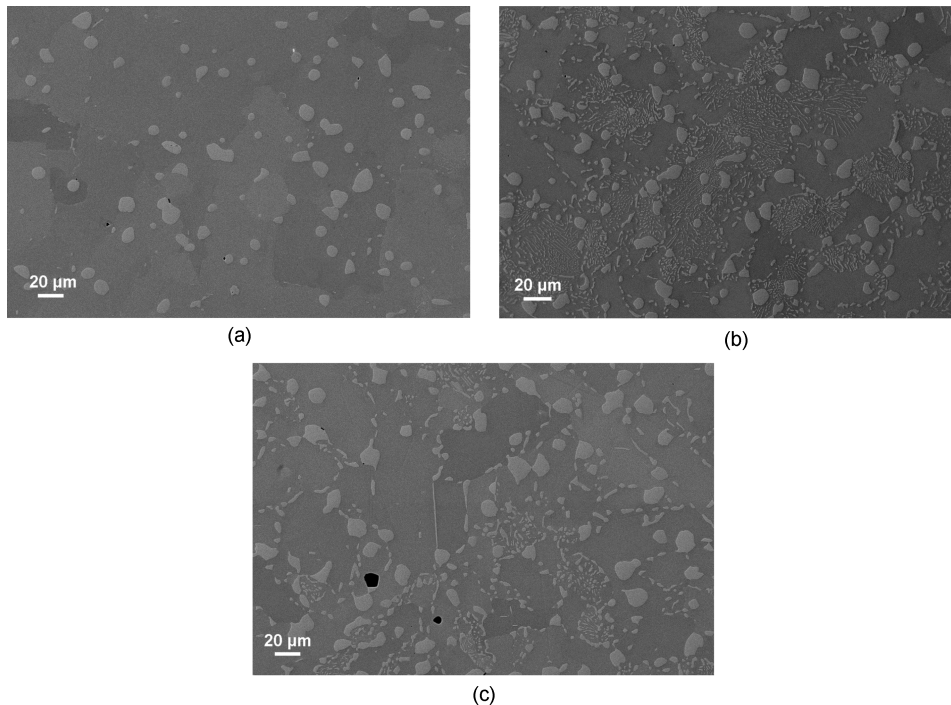


Fig. 6 SEM images showing the  $\sigma$  phase morphology in Co-17Re-23Cr alloy after different heat treatments: (a) ST, (b) ST + 1000°C/100 h/WQ and (c) ST + 1100°C/100 h/WQ

In Fig. 6 the microstructure of the Co-17Re-23Cr+200B alloy is presented and it shows the  $\sigma$  phase morphology typical of all Co-17Re-23Cr type alloys with or without B additions. In the ST condition the  $\sigma$  phase is present mostly as large particles at grain boundaries and some within the grains (Fig. 6a). The Co-17Re-23Cr alloy (i.e., the alloy without B) contains only ~2% of  $\sigma$  phase (area fraction measured on SEM images in ST condition) as can be seen from the plot in Fig. 7. However, in alloys with B addition (50 to 1000 wt. ppm) the amount of  $\sigma$  phase is somewhat higher (~8%) after the same heat treatment condition (Fig. 7). The  $\sigma$  phase morphology is not affected by B addition and also the  $\sigma$  amount remains more or less independent of the actual B content in the alloy after the ST heat treatment. However, additional  $\sigma$  phase precipitates on further exposure of the alloys at 1000° and 1100°C and these secondary  $\sigma$  precipitates are much finer in size. After cooling from 1000°C the  $\sigma$  phase is obtained in the form of lamellae (Fig. 6b), while they are somewhat equiaxed (but still very fine) after cooling from 1100°C (Fig. 6c). The additional precipitation of  $\sigma$  phase results in an increase of the volume fraction and the measured total  $\sigma$  fraction more than doubles compared to that in the ST condition (Fig. 7). The plot in Fig. 7 includes data from samples exposed for 100 and 300 h at 1000° and 1100°C and it can be seen that the  $\sigma$  phase is quite stable and its morphology and volume remain stable even after the long exposures at the high temperatures. However, in alloys with boron content equal to or greater than 500 ppm the amount of fine secondary  $\sigma$  precipitates is much less. It is apparent that the precipitation of larger amount of Cr-Re rich borides in alloys with higher boron restricts the availability of Cr and Re for the formation of secondary  $\sigma$  precipitates. However, in all alloys a

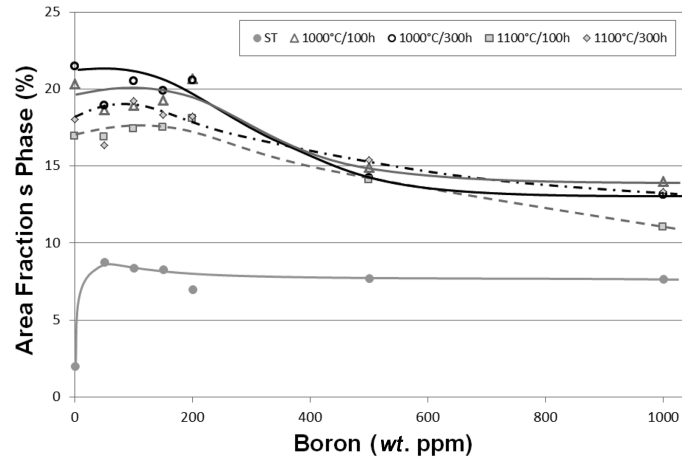


Fig. 7 Volume fraction of  $\sigma$  phase in ST condition and after 100 and 300 h hold time at 1000° and 1100°C

significant amount of secondary  $\sigma$  precipitate form on exposure to high temperatures and thereby affect the structural stability. In order to avoid such instability and produce a stable microstructure during high temperature applications a stabilizing ageing heat treatment (1000°C / 24 h / air cool) is introduced in the Co-17Re-23Cr base alloys.

#### 4. Stability of TaC precipitates

The mono-carbide (TaC) of the Group V A transition metal *Ta* is exploited as a hardening precipitate by adding *Ta* and *C* in the Co-17Re-23Cr-1.2*Ta*-2.6*C* alloy designated here as CoRe-2. A boron added variation of the alloy CoRe-2 with 200 wt. ppm *B* is named CoRe-2*B*. The alloys have complex microstructures with multiple phases in different morphologies and in different length scales (Gilles 2012). The microstructures observed at low magnification in the two alloys (CoRe-2 and CoRe-2*B*) in ST condition are very similar and consist of large equiaxed  $\sigma$  phase particles (> 20  $\mu\text{m}$ ) and Chinese Script (CS) like TaC particles at the grain boundaries and somewhat smaller (~ 0.5 to 10  $\mu\text{m}$ ) round TaC and  $\sigma$  phase particles within the grains. In addition there is a finer structure within the grains which is quite different in the two alloys. While the CoRe-2 alloy contains fine lamellae of  $\text{Cr}_{23}\text{C}_6$  type carbides (~200 nm thick) in the hcp Co-matrix grains, the CoRe-2*B* alloy contains a fine dispersion of  $\sigma$  phase particles (~500 nm) after a similar heat treatment (Gilles 2012). Furthermore, there exists an even finer structure in both the alloys which is typically represented by the in-lens SEM image from CoRe-2 alloy in Fig. 8. The fine particles in Fig. 8 have been identified as TaC by X-ray and electron diffraction and have a mean size of 20-50 nm depending on the alloy or the heat treatment. This very fine dispersion of TaC carbide constitutes an ideal microstructure for high temperature creep resistance. In CoRe-2 alloy it was found that the fine *Ta*-carbide precipitates interact with dislocations during high temperature creep deformation (Depka *et al.* 2009, Brunner *et al.* 2010).

To characterize the fine TaC precipitates in both the alloys, in-situ high energy small angle X-ray scattering (SAXS) and diffraction measurements were carried out with synchrotron radiation at the

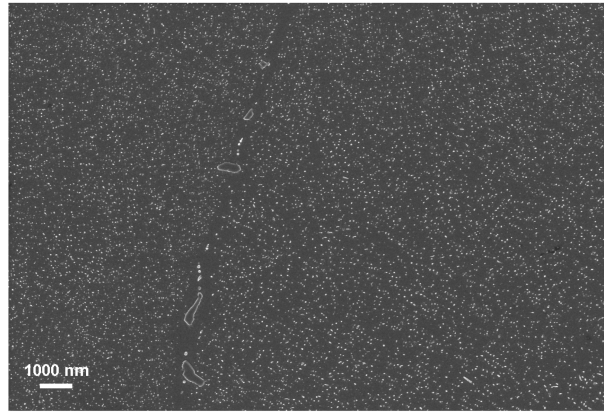


Fig. 8 In-lens SEM image from CoRe-2 alloy showing the very fine dispersion of TaC particles in the microstructure

Engineering Materials Science Beamline HARWI-II (Lippmann 2007) at HZG outstation at the Deutsches Elektronen-Synchrotron (DESY) in Hamburg, Germany. For the heating experiment, a dilatometer (Bähr 805 *A/D*) was used. Cylindrical samples with a diameter of 3 mm and a length of 12 mm were heated up to 1350°C with a rate of 100 K/min, held for short time at 1280°C, 1200°C and 1100°C respectively and then cooled down to room temperature at a similar rate. Monochromatic synchrotron radiation of  $0.7 \times 0.7$  mm with a nominal energy of 100 keV was used for all measurements. SAXS and diffraction patterns were recorded continuously during heating, holding of temperature and cooling on an image plate detector (MAR 555, with a resolution of  $3072 \times 2560$  pixels) at a sample to detector distance of 8725 mm (SAXS) and 1837 mm (diffraction) respectively. An exposure time of 2 s was chosen for each measurement. The intensities from diffraction spots in a ring were azimuthally integrated to obtain the one dimensional diffractogram. Selected diffractograms from these measurements on Co-Re alloys are presented in Fig. 9 and Fig. 10. Fig. 9 shows diffractograms from CoRe-2 and CoRe-2B sample in ST condition measured at RT. In both CoRe-2 and CoRe-2B the presence of many different phases namely,  $\epsilon$  Co (hcp),  $\gamma$  Co (fcc), TaC,  $\text{Cr}_{23}\text{C}_6$  and  $\sigma$  phase could be identified. The corresponding peaks of all the identified phases in the diffractograms are indexed in Fig. 9 which shows that both the alloys have the same phases present and only their volume fraction differs. However, the microstructural evidence showed the presence of additional  $\text{Cr}_2\text{B}$ -type boride particles at the grain boundaries in CoRe-2B alloy (Gilles *et al.* 2012). This phase could not be detected in the diffraction results, possibly due to its very low volume fraction. Fig. 10 shows that TaC phase is stable at 1300°C and the Co matrix has hcp ( $\epsilon$ ) structure at low temperatures and fcc ( $\gamma$ ) structure at high temperatures.

Simultaneous measurement of diffraction and dialotometry was performed in-situ during the heating / cooling cycle. Fig. 11 shows the dilatometer plot during in-situ heating of the CoRe-2 alloy from RT to 1350°C @ 1 K/s. The diffraction data recorded on the 2D area detector at selected temperatures are also shown in this figure to emphasize the observed  $\epsilon_{\text{hcp}}$  to  $\gamma_{\text{fcc}}$  phase transformation of the Co-matrix phase. The temperature ranges over which the secondary  $\sigma$  phase forms and the hcp to fcc transformation occurs were determined from the dilation and the diffraction data and these regions are highlighted in Fig. 11. In the 2D diffraction patterns the main peaks from the Co matrix (hcp and / or fcc) are indicated.

In situ SAXS measurements allowed monitoring the stability of fine TaC precipitates at high

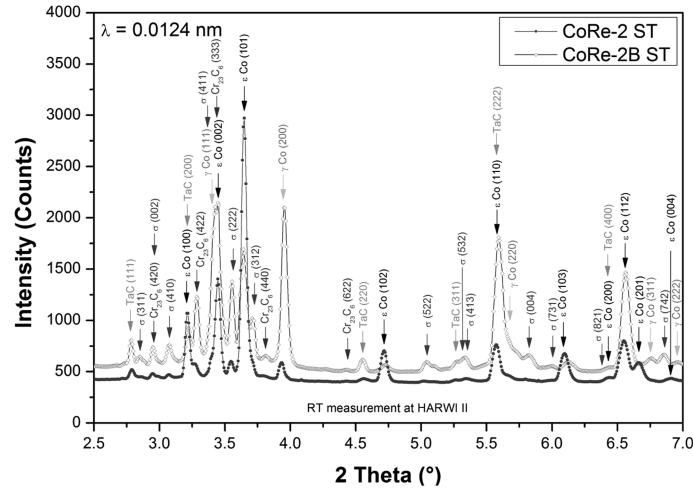


Fig. 9 The diffractograms measured on CoRe-2 and CoRe-2B alloys at RT shows the presence of many different phases in the two alloys, namely,  $\epsilon$  Co (hcp),  $\gamma$  Co (fcc), TaC,  $\text{Cr}_{23}\text{C}_6$  and  $\sigma$  phase. The corresponding peaks of all the phases are indexed. Additionally, in the CoRe-2B alloy a Cr, Re rich  $\text{Cr}_2\text{B}$ -type boride phase is present, but due to its small volume fraction the peaks from this phase could not be detected

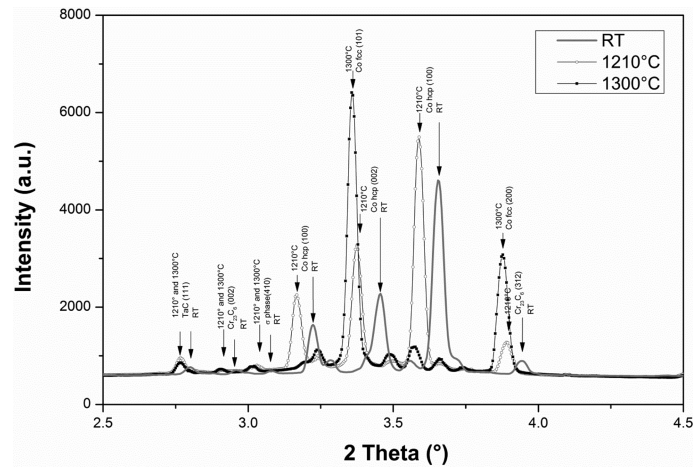


Fig. 10 Selected diffractograms from CoRe-2 alloy in limited 2 Theta angular range measured at 1210° and 1300°C are compared with the measurement at RT. It shows the Co matrix transformations from the low temperature  $\epsilon$  (hcp) structure to the high temperature  $\gamma$  (fcc) structure between 1210° and 1300°C. Only some peaks of the TaC,  $\text{Cr}_{23}\text{C}_6$  and  $\sigma$  phases are indexed in this figure

temperatures and the kinetics of precipitate coarsening during the heating/cooling and the short hold times. The heating / cooling cycle of the SAXS and the diffraction experiments were kept identical. The intensities were normalized to the X-ray flux and corrected for background scattering, transmission and polarisation by using the software package FIT2D (Hammersley *et al.* 1996). As the scattering profile was generally symmetric, the intensity  $I(q)$  versus scattering vector were

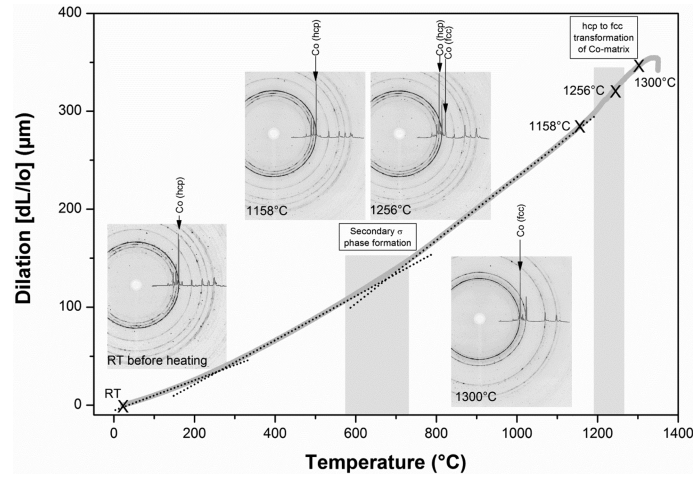


Fig. 11 Shows a dilatometer plot during in-situ heating of the CoRe-2 alloy from RT to 1350°C @ 1 K/s. The diffraction data recorded on the 2D area detector at selected temperatures are also shown in this figure where the major Co hcp and fcc peaks are indicated. The temperature region where secondary σ phase forms and the Co-matrix hcp to fcc transformation occurs were are highlighted in the figure

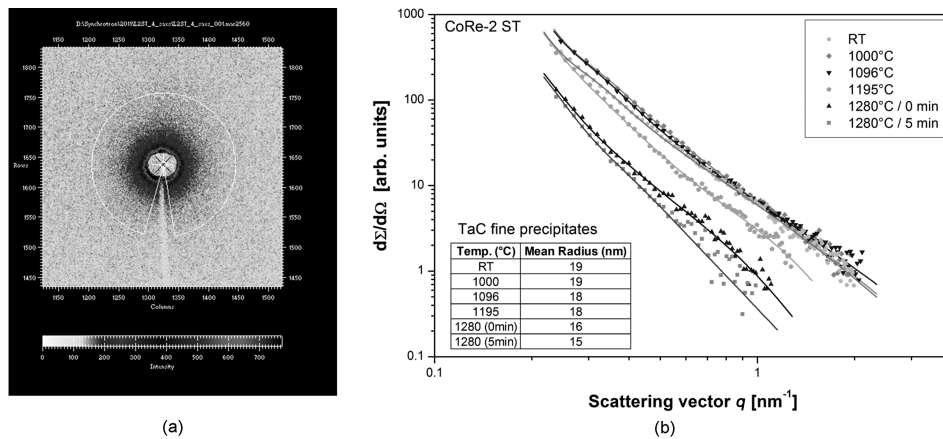


Fig. 12 (a) A typical scattering profile recorded on the area detector is shown. The data was azimuthally averaged over the marked angular region to avoid the influence of the beam-stop and (b) The measured SAXS data from CoRe-2 alloy at selected temperatures and the fitted data in the measured  $Q$  range are plotted. The particle size distribution of the fine TaC precipitates where determined from the SAXS results and the mean particle radius of the TaC particles at different temperatures are listed as inset in the figure

extracted by azimuthally averaging circular sectors and then integrating (Fig. 12a). The resulting cross-sectional data from the CoRe-2 alloy at selected temperatures are plotted against scattering vector  $Q$  (Fig. 12b). The data analysis provided the particle size distribution (PSD) of the fine TaC precipitates and their evolution during in-situ cycling. The corresponding mean particle size results are listed as inset in Fig. 12b. It is clear from the diffraction results (e.g. the (111) TaC peak intensity in Fig. 10) that the TaC phase remains stable up to 1300°C.

## 5. Discussions

Both the strengthening concepts presented here, namely precipitation hardening by MC type *Ta*-carbides and strengthening of grain boundaries by addition of boron was quite effective at room temperature and this provided high strength to the matrix with sufficient ductility. Very small amount of *B* addition (50 to 1000 *wt. ppm*) to the polycrystalline Co-Re alloys has a profound effect on both room and high temperature strength and ductility of the Co-17Re-23Cr alloys. From the present and earlier studies (Mukherji *et al.* 2012b, Böllitz *et al.* 2012) there is evidence of *B* segregation to the grain boundaries. In fact even the smallest *B* addition of 50 ppm stabilizes Cr<sub>2</sub>B-type borides at the grain boundaries in Co-Re alloys. The boride phase fraction increases with the amount of boron addition to the alloy and more and more grain boundaries are decorated with boride particles. The hardness results (Fig. 4) show that at RT, the alloy strength peaks at about 200 ppm *B*. Further, boron addition enhances the grain boundary cohesiveness and changes the fracture mode. The ductility is actually maximised for the alloy with 500 ppm *B* addition (Mukherji *et al.* 2012b). It is therefore apparent that the presence of Cr-borides at grain boundaries may not be the primary reason for the improvement in strength and ductility. However, presence of elemental boron could not be detected at grain boundaries by EELS, other than within the Cr<sub>2</sub>B-type particles (Böllitz *et al.* 2012).

In Ni-based superalloys segregation of boron at grain boundaries has been confirmed by advanced techniques such as secondary ion mass spectroscopy (e.g. Thuvander and Stiller 2000), atom-probe / 3D atom-probe (e.g. Cadel *et al.* 2002) and neutron induced radiography (Kim *et al.* 1997) and the boron addition is restricted to the limit where the borides do not form. Measurements by 3D atom probe and neutron induced  $\alpha$ -track mapping on the Co-17Re-23Cr + *B* alloys are on-going and at this point it is not clear if elemental boron is present at the grain boundaries or not. However, the first results from the  $\alpha$ -track mapping on alloys with carbide precipitates show evidence of *B* segregation at the grain boundaries for some carbide containing Co-Re-Cr alloy compositions only (e.g. in CoRe-2 alloy containing TaC carbides). In other alloys (e.g. in CoRe-1<sup>3</sup> alloy with Cr<sub>23</sub>C<sub>6</sub> carbides) there are indications that boron is also distributed within the grains and interacts with the Cr-carbides. The results from the spatially resolved neutron induced radiography measurement will be published elsewhere (Mukherji *et al.* 2012c) and will provide information such as, under what circumstances the elemental boron segregates to the grain boundaries. At this point it suffices to say that in the alloy series Co-17Re-23Cr+*B* the borides at the grain boundaries cannot be the main source of strengthening or ductility enhancement. This is because in that case the alloy with the highest boron content (Co-17Re-23Cr+1000*B*) having most grain boundaries decorated with Cr<sub>2</sub>B-type boride particles should have shown the best properties in terms of strength and ductility, but this is clearly not the case. Further, it is clear that addition of boron in excess of 200 *wt. ppm* is not more beneficial and also affects the formation of the secondary  $\sigma$  phase precipitates. Very low amount of boron addition (<100 *wt. ppm*) also does not provide sufficient strengthening, although unlike the Ni-superalloys even 50 ppm *B* is sufficient to stabilize some Cr<sub>2</sub>B-type boride in Co-Re alloys. About 150 to 200 *wt. ppm B* is apparently the optimal amount for the Co-Re alloys.

Although, the microstructure of carbide containing CoRe-2 alloys is very complex with the presence of many different phases in different morphologies, a fine dispersion of TaC precipitates (Fig. 8) could be obtained through suitable heat treatment in both CoRe-2 and CoRe-2*B* alloys. Such fine precipitate structure is suitable from the point of view of creep strengthening and it was

---

<sup>3</sup>Composition of CoRe-1 is Co-17Re-23Cr-2.6C

also found that the TaC particles do in fact interact with the dislocation and hinder their motion (Depka *et al.* 2009). The stability of the microstructure at the creep deformation temperatures is however, also extremely important. The results of in-situ measurements with neutron and synchrotron in the temperature range 1000° to 1300°C and the SAXS results presented here shows that although the fine TaC precipitates coarsens, they still remain quite fine on exposure up to 1280°C. In-situ measurements are very useful and they provided information of the precipitate morphology at the temperature. However, such studies can only provide results after short time exposures due to the resource limitations for conducting long term exposure studies in large experimental facilities. Therefore, additional ex-situ experiments of long time exposures and diffraction and microstructural measurements are necessary. Such studies were also conducted on CoRe-2 and CoRe-2B alloys with X-ray diffraction and electron microscopy and the results will be presented in an upcoming publication (Gilles *et al.* 2012). However, it shows that the TaC precipitates size remains fine (<50 nm) even after exposure of up to 100 h at 1200°C. Finally, it is seen that boron addition to CoRe-2 alloy does change the microstructure and stabilize additional boride phase, but it does not affect the dispersion of the fine TaC precipitates and their stability. It should therefore be possible to combine the two strengthening mechanisms – e.g. precipitate strengthening by TaC and grain boundary strengthening through boron additions.

## **6. Conclusions**

Co-Re based alloys show promise as a new class of high temperature alloy. However, much work is still needed before a technical alloy will be available for structural applications. Microstructural studies and in situ measurements at high temperatures with synchrotron radiation were used to investigate the high temperature stability of the hardening TaC precipitates in experimental Co-Re-base alloys. Results show that TaC precipitates can be finely dispersed in Co-Re-Cr-Ta-C alloys through suitable heat treatments and these precipitates can remain generally stable on high temperature exposures.

At present the Co-Re alloy development work is concentrating on polycrystalline alloys and it was found that grain boundary embrittlement is an issue. However, this could be effectively addressed through addition of small amount of boron to Co-Re alloys. Unlike in Ni-alloys, some Cr-Re-rich borides form in Co-Re alloys, even for very small addition of 50 *wt. ppm B*. However, it appears that boron in elemental form and not the borides at the grain boundaries provide the strength and ductility. This however, needs further confirmation. The present result shows that an addition of 150 to 200 *wt. ppm B* is optimal for the Co-17Re-23Cr experimental alloy from the point of strength and ductility at RT.

## **Acknowledgements**

We would like to thank the German Research Foundation (DFG) for financial support of this research in the frame of the DFG Forschergruppe program (FOR 727): “Beyond Ni-base Superalloys”. Further, we thank T. Fischer for providing assistance at the HARWI-II beamline and Dr S. Piegert for the thermodynamic calculations. We also gratefully acknowledge the financial support provided by Helmholtz-Zentrum Geesthacht for the beam time at DESY.

## References

- Bölitz, M.C., Brunner, M., Völkl, R., Mukherji, D., Roesler, J. and Glatzel, U. (2012), "Microstructural study of Boron-doped Co-Re-Cr alloys by means of transmission electron microscopy and electron energy loss spectroscopy", *Int. J. Mater. Res.*, **103**(5), 554-558.
- Brunner, M., Hüttner, R., Bölitz, M.C., Völkl, R., Mukherji, D., Rösler, J., Depka, T., Somsen, Ch., Eggeler, G. and Glatzel, U. (2010), "Creep properties beyond 1100°C and microstructure of Co-Re-Cr alloys", *Mater. Sci. Eng.*, **528**, 650-656.
- Cadel, E., Lemarchand, D., Chambrel, S. and Blavette, D. (2002), "Atom probe tomography investigation of the microstructure of superalloys N18", *Acta Mater.*, **50**(5), 957-966.
- Depka, T., Somsen, C., Eggeler, G., Mukherji, D., Rösler, J., Krüger, M., Saage, H. and Heilmaier, M. (2009), "Microstructures of Co-Re-Cr, Mo-Si and Mo-Si-B high-temperature alloys", *Mater. Sci. Eng.*, **510-511**, 337-341.
- Gilles, R., Mukherji, D., Strunz, P., Hofmann, M., Hoelzel, M., Barbier, B., Euler, H., Roesler, J. and Gasser, U. (2012), "Stability and coarsening of TaC precipitates in Co-Re-Cr based alloy being developed for ultra-high temperature applications", *Acta Mater.*, Submitted.
- Gorr, B., Trindade, V., Burk, S., Christ, H.J., Klauke, M., Mukherji, D. and Rösler, J. (2009), "Oxidation behaviour of model cobalt-rhenium alloys during short-term exposure to laboratory air at elevated temperature", *Oxid. Met.*, **71**(3-4), 157-172.
- Hammersley, A.P., Svensson, S.O., Hanfland, M., Fitch, A.N. and Häuser, D. (1996), "Two-dimensional detector software: From real detector to idealised image or two-theta scan", *High Pressure Res.*, **14**(4), 235-248.
- Heilmaier, M., Krüger, M., Saage, H., Rösler, J., Mukherji, D., Glatzel, U., Völkl, R., Hüttner, R., Eggeler, G. Somsen, Ch., Depka, T., Christ, H.J., Gorr, B. and Burk, S. (2009), "Current development status of metallic materials for structural applications beyond nickel base superalloys", *Jom.-US*, **61**(7), 61-67.
- Kim, H.J., En, Z., Ho, J.H., Jang, J.S., Jurneav, N. and Usmanova, M.M. (1997), "Boron distribution measurement in metals by neutron induced radiography", *J. Radioanal. Nucl. Ch.*, **216**(1), 117-120.
- Klauke, M., Mukherji, D., Gorr, B., Christ, H.J. and Rösler, J. (2009), "Oxidation behaviour of experimental Co-Re-base alloys in laboratory air at 1000°C", *Int. J. Mater. Res.*, **100**, 104-111.
- Lippmann, T., Lottermoser, L., Beckmann, F., Martins, R.V., Dose, T., Kirchhof, R. and Schreyer, A. (2007), "New developments at the engineering materials science beamline HARWI II", *HASYLAB annual report 2007*, Caliebe, W., Drube, W., Rickers, K., Schneider, J.R. (Eds.), HASYLAB/DESY, Hamburg.
- Lukas, H., Fries, S.G. and Sundman, Bo. (2007), *Computational thermodynamics: The calphad method*, Cambridge University Press, Cambridge, UK.
- Massalski, T.B. (1986), *Binary alloy phase diagrams*, **1**, ASM, Ohio.
- Miller, S. (1996), "Advanced materials mean advanced engines" Abstracted from *Materials World*, **4**, 446-449. [www.azom.com/details.asp?ArticleID=90](http://www.azom.com/details.asp?ArticleID=90)
- Mukherji, D., Klauke, M., Strunz, P., Zizak, I., Schumacher, G., Wiedenmann, A. and Rösler, J. (2010a), "High temperature stability of Cr-carbides in an experimental Co-Re-based alloy", *Int. J. Mater. Res.*, **101**, 340-348.
- Mukherji, D. and Rösler, J. (2010b), "Co-Re-based alloys for high temperature applications: Design considerations and strengthening mechanisms", *J. Phys. Conf. Series*, **240**(1), 012066.
- Mukherji, D., Strunz, P., Gilles, R., Hofmann, M., Schmitz, F. and Rösler, J. (2010c), "Investigation of phase transformations by in-situ neutron diffraction in a Co-Re-based high temperature alloy", *Mater. Lett.*, **64**, 2608-2611.
- Mukherji, D., Rösler, J., Fricke, T., Piegert, S. and Schmitz, F. (2010d), "New concept of composite strengthening in Co-Re-based alloys for high temperature applications in gas turbines", *Proceedings of 9th Liège Conference on Materials for Advanced Power Engineering*, Lecomte, J., Contrepois, Q., Beck, T. and Kuhn, B. (Eds.), Energy & Environment, Vol 94, Jülich Forschungszentrum, ISBN 978-3-89336-685-9.
- Mukherji, D., Strunz, P., Piegert, S., Gilles, R., Hofmann, M., Hölzel, M. and Rösler, J. (2012a), "The hcp-fcc transition in co-re-based experimental alloys investigated by neutron scattering", *Metall. Mater. Trans. A*, published online, DOI: 10.1007/s11661-011-1058-4.
- Mukherji, D., Rösler, J., Krüger, M., Heilmaier, M., Bölitz, M.C., Völkl, R., Glatzel, U. and Szentmiklósi, L. (2012b), "Effects of boron addition on microstructure and mechanical properties of Co-Re based high

- temperature alloys”, *Scripta Mater.*, **66**, 60-63.
- Mukherji, D., Szentmiklósi, L., Zsuzsi, M. and Rösler, J. (2012c), “Mapping surface boron density distribution in Co-Re alloys with neutron induced a track mapping” – in preparation.
- Okamoto, H. (2003), “Co-Cr (Cobalt-Chromium)”, *J. Phase Equilib. Diff.*, **24**, 377-378.
- Perepezko, J.H. (2009), “The hotter the engine, the better”, *Science*, **326**, 1068-1069.
- Reed, R.C. (2006), *The Superalloys: fundamentals and applications*, Cambridge University Press, Cambridge.
- Rösler, J., Mukherji, D. and Baranski, T. (2007), “Co-Re-based alloys: A new class of high temperature materials?”, *Adv. Eng. Mater.*, **9**(10), 876-881.
- Sato, J., Omori, T., Oikawa, K., Ohnuma, I., Kainuma, R. and Ishida, K. (2006), “Cobalt-base high-temperature alloys”, *Science*, **312**, 90-91.
- Sokolovskaya, E.M., Tuganbaev, M.L., Stepanova, G.I., Kazakova, E.F. and Sokolova, I.G. (1986), “Interaction of cobalt with chromium and rhenium”, *J. Less-Common Metals*, **124**, 5-7.
- Thuvander, M. and Stiller, K. (2000), “Microstructure of a boron containing high purity nickel-based alloy 690”, *Mater. Sci. Eng.*, **281**(1-2), 96-103.